PHYSICAL REVIEW B **77**, 201408(R) (2008)

Deriving molecular bonding from a macromolecular self-assembly using kinetic Monte Carlo simulations

Fabien Silly,[1,2,*] Ulrich K. Weber,[1] Adam Q. Shaw,[1] Victor M. Burlakov,[1,3,†] Martin R. Castell,[1] G. A. D. Briggs,[1] and David G. Pettifor[1]

[1]*Department of Materials, University of Oxford, Parks Road, Oxford OX1 3PH, United Kingdom*

[2]*Zernike Institute for Advanced Materials, University of Groningen, Nijenborgh 4, NL-9747 AG Groningen, The Netherlands*

[3]*Institute for Spectroscopy, Russian Academy of Sciences, Troitsk 142190, Russia*

(Received 11 April 2008; published 29 May 2008)

Macromolecules can form regular structures on inert surfaces. We have developed a combined empirical and modeling approach to derive the bonding. From experimental scanning tunneling microscopy images of structures formed on Au(111) by melamine, by 3,4,9,10-perylene-tetracarboxylic-dianhydride, and by a 2:3 mixture of the two, we determine the molecular bonding morphologies. Within these bonding morphologies and by recognizing the distinction between cohesive and adhesive molecular interactions, we simultaneously simulated different molecular structures by using a lattice Monte Carlo method.

DOI: 10.1103/PhysRevB.77.201408 PACS number(s): 81.07.Nb, 05.10.Ln, 68.37.Ef, 81.16.Dn

Self-assembly of molecules on atomically well-defined surfaces offers a bottom-up approach for generating two-dimensional nanostructures.[1–15] To develop structures for specific purposes requires a precise knowledge of the molecular bonding, including molecular binding rules and the corresponding binding energies.[16,17] These cannot always be calculated *ab initio* because of the complex character of molecular bonding and the difficulty of including dispersive (van der Waals) interactions.[18]

Hydrogen bond-forming molecules are particularly suitable for generating self-assembled structures due to the high selectivity and directionality of hydrogen bonds[20–22] and relatively low energetics, which enable equilibrium molecular configurations to be achieved at relatively low processing temperatures.[9,19] Using mixtures of different hydrogen bond-forming molecules, with diverse binding rules,[23,24] allows the formation of a wider variety of molecular structures by changing molecular composition, and presents a promising approach to generating molecular scaffolds.[26] The relation between the properties of individual molecules and the characteristics of their self-assembly on surfaces remains to be understood. Our study provides a step toward establishing such a relation by solving the inverse problem—extracting characteristics of molecular interactions by analyzing self-assembled structures.

As part of the objective of this Rapid Communication, we use experimental observations of a self-assembled molecular structure to determine plausible binding rules, and then perform kinetic Monte Carlo simulations to estimate the binding energies. We simultaneously analyze the structural stability of the stoichiometric molecular mixture and the individual constituent molecular components. We apply this methodology to 3,4,9,10-perylene-tetracarboxylic-dianhydride (PTCDA) and melamine molecules on Au(111), where the substrate has little effect on intermolecular interactions.

Our procedure for extracting the molecular binding rules and the corresponding interaction energies involves two major steps. In the first step, we analyze experimentally observed molecular structures in order to extract the characteristics of the molecular arrangement for all molecular compositions of interest. Thereby, we identify the ways molecules bind to each other, i.e., the molecular binding rules. We assume that the role of the metallic substrate is limited to constraining the molecular system in two dimensions, which is a good approximation for noble metal substrates. In the second step, we construct the model system by using the binding rules and arranging the molecules on a grid, suitable for on-lattice kinetic Monte Carlo simulations of molecular structures. Thereby, we extract the molecular binding energies by simultaneously analyzing the stability of both the single-component molecular structures and of that formed from a binary mixture.

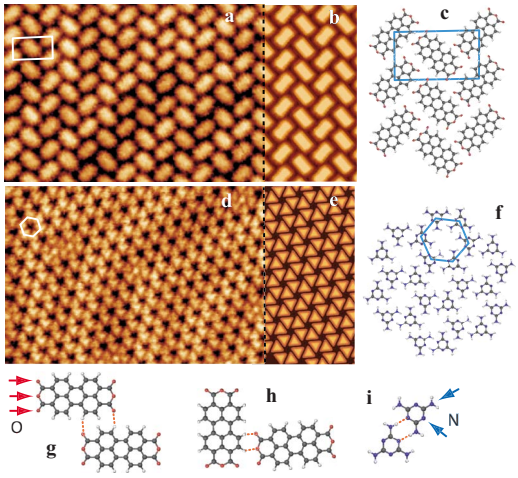

FIG. 1. (Color online) [(a)–(c)] PTCDA domain: (a) STM image on Au(111) surface (14×10 nm^2; $V_s=+1.5$ V, $I_t=0.4$ nA), (b) simulation result displayed on a sheared hexagonal lattice, and (c) molecular ordering. [(d)–(f)] Melamine domain: (d) STM image (14×10 nm^2; $V_s=-1.0$ V, $I_t=0.5$ nA), (e) simulation shown on a simple hexagonal lattice, and (f) molecular ordering. The unit cell is outlined in blue (gray). [(g), (h), and (i)] Plausible molecular bonds occurring in structures (c) and (f). In the molecule 3D representation, dark gray balls are carbon atoms, red (light gray) balls are oxygen atoms, white balls are hydrogen atoms, and blue (gray) balls are nitrogen atoms. Red (light gray) arrows in (b) point at oxygen atoms (O) of PTCDA molecule and blue (gray) arrows in (i) point at nitrogen atoms (N) of melamine molecule.

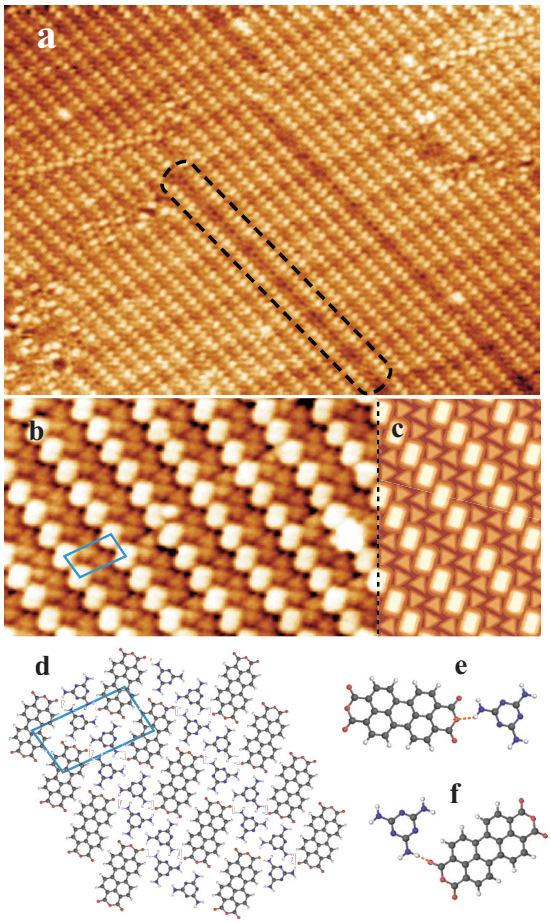

FIG. 2. (Color online) Mixed PTCDA and melamine domain. (a) STM image on Au(111) surface (80×60 nm^2; $V_s=-1.2$ V, $I_t=0.2$ nA). (b) Close up (14×8 nm^2; $V_s=-1.5$ V, $I_t=0.1$ nA). (c) Simulation result shown on a sheared hexagonal lattice. (d) Model of the molecular ordering. [(e) and (f)] Plausible molecular bonds occurring in (d).

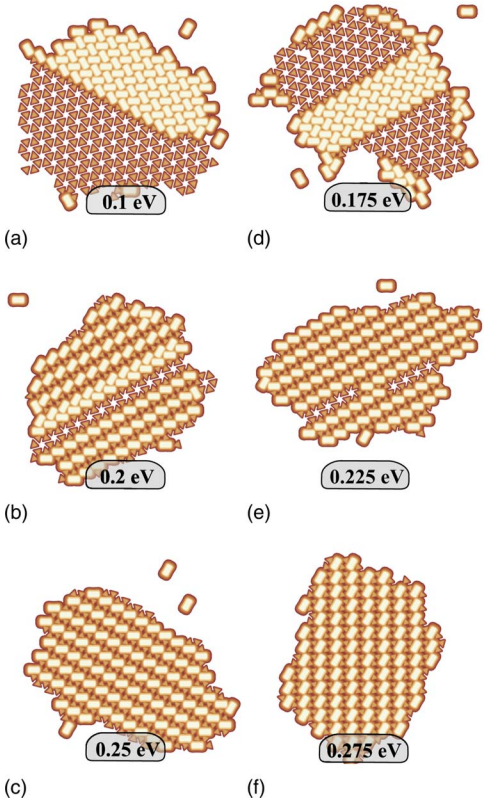

FIG. 3. (Color online) Simulated PTCDA-melamine ordering depending on PTCDA-melamine bond energies $E_{mp}^{(1)}=E_{mp}^{(2)}=E_{\mathrm{ad}}$, which vary from 0.1 to 0.275 eV. [(a) and (b)] Small bond energies between PTCDA and melamine with $E_{\mathrm{ad}}\leqslant0.175$ lead to phase segregation. [(c) and (d)] In a narrow energy range of $0.2\leqslant E_{\mathrm{ad}}\leqslant0.225$, melamine double rows can be observed as a typical defect. [(e) and (f)] Energies $E_{ad}\geqslant0.25$ allow the formation of a defect-free PTCDA-melamine domain.

We used Au(111) film grown on mica substrates. The samples were introduced into the ultrahigh vacuum (UHV) chamber of a scanning tunneling microscope (STM) (JEOL JSTM4500S) operating at a pressure of 10^{-8} Pa. The Au(111) surfaces were sputtered with argon ions and annealed in UHV at temperatures between 600 and 800 °C typically for 30 min. PTCDA molecules were sublimated at 275 °C and melamine at 100 °C. Electrochemically etched tungsten tips were used to obtain constant current (I_t) images at room temperature with the bias voltage (V_s) applied to the sample. The structure of the molecular mixture was obtained after deposition of PTCDA on Au(111), followed by a deposition of melamine with a 2:1 ratio and a post annealing at 90 °C for 10 h. STM images have been processed and analyzed with FABVIEWER.[25]

Molecular binding rules between identical molecules are obtained by comparing the molecular arrangements in the single-component molecular structures. The experimental images of the molecular structures of PTCDA and 1,3,5-triazine-2,4,6-triamine (melamine) self-assembled on Au(111) are shown in Fig. 1. Figure 1(a) shows the compact domains of PTCDA, which exhibit a uniform structure with a herringbonelike pattern. The 12.0×20.0 Å^2 unit cell of the structure is rectangular and contains two molecules, with their main axes oriented at an angle of 86° with respect to each other.[27] Molecular bonding in the PTCDA structure can be characterized by two independent parameters $E_{pp}^{(1)}$ and $E_{pp}^{(2)}$, as illustrated in Figs. 1(g) and 1(h), respectively. Melamine molecules on Au(111), according to Fig. 1(d), form domains of chiral structure and hexagonal symmetry with the lattice parameter of 9.8 Å. This arrangement is stabilized by a double hydrogen bond,[28] as illustrated in Fig. 1(i). The corresponding energy E_{mm} for the melamine-melamine bonding is found to be $E_{mm}=0.45$ eV.[29]

Details of the melamine-PTCDA molecular bonding are obtained by analyzing the structure of the melamine-PTCDA mixture with the composition 2:1. This large scale structure is formed of ordered molecular stripes, as shown in Fig. 2(a). Each stripe is composed of a single PTCDA molecular row and a double row of melamine molecules [Fig. 2(b)]. The PTCDA molecular axis is rotated 50° with respect to the stripe line, thereby making this structure chiral. The unit cell outlined in Fig. 2(b) in blue (gray) has a parallelogram shape, with an angle of 85° with 10.0 Å (the periodicity along the PTCDA rows) and 19.9 Å parameters (PTDCA-PTCDA separation across two melamine rows). Figure 2(d)

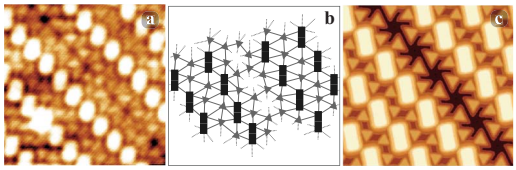

FIG. 4. (Color online) The double melamine row in a PTCDA-melamine domain. (a) Close-up of a STM image (8×8 nm^2; $V_s=-1.2$ V, $I_t=0.2$ nA). (b) Scheme showing the common topology of both experiment and simulation. Black rectangles are PTCDA molecules and gray triangles are melamine molecules. (c) Simulated image using a simple hexagonal geometry.

shows the molecular arrangement as observed in Fig. 2(b). Molecular interactions in the PTCDA-melamine structure can, in general, be characterized by two parameters $E_{mp}^{(1)}$ and $E_{mp}^{(2)}$ corresponding to physically reasonable hydrogen bonding, as illustrated in Figs. 2(e) and 2(f).

The molecular binding energies $E_{pp}^{(1)}$, $E_{pp}^{(2)}$, $E_{mp}^{(2)}$, and $E_{mp}^{(2)}$ can now be estimated by studying the stability of the self-assembled single components and the mixed molecular structure using the kinetic Monte Carlo methodology,[29] with an underlying hexagonal grid defining the topology of molecular movements and interactions and an (N,V,T) ensemble.

The on-lattice kinetic Monte Carlo model is an entirely topological model. It exclusively considers binding energies between molecules that are nearest neighbors in the underlying lattice and does not contain information about the absolute position and orientation of molecules. Therefore, the point of comparison between experimental and simulated structures is the topological correspondence (Fig. 4). The freedom to apply different geometries to a simulation while keeping the topology unchanged can be used for visualization of highly ordered homogeneous molecular arrangements (Figs. 1 and 2), where a sheared hexagonal geometry achieves good correspondence. In other cases where the geometry is more complex due to defects or irregularities (Figs. 3 and 4), the simulation is presented with a simple hexagonal geometry. In each case, what matters is the correspondence in topology between simulation and experiment.

In our simulations, we use a binary mixture of anisotropic molecules of type 1 (trigonal vertices) and type 2 (linear rods) occupying one and two sites, respectively, on a 30×30 two-dimensional hexagonal lattice, initialized in a random configuration. Rodlike molecules exist in three different orientations along the symmetry axes of the hexagonal grid, while vertexlike molecules exist in two different orientational configurations due to their twofold and threefold molecular symmetries. Any pair of molecules that exists in one of the nearest neighbor configurations, shown in Figs. 1(g)–1(i), 2(e), and 2(f), establishes a hydrogen bond with the energies E_{mm}, $E_{pp}^{(1,2)}$, $E_{pp}^{(1,2)}$, respectively. The number of molecules (200 vertices and 100 rods) is chosen to be stoichiometric, which complies with the ratio of the experimentally observed unit cell shown in Fig. 2. The simulation temperature of $k_BT=0.08$ eV is higher than in experiment to enable short equilibration times, but low enough to avoid thermally generated defects.

In our simulations, we neglect the influence of the substrate on the molecular binding energies, which is a reasonable approximation for the PTCDA and melamine molecules on Au(111).[30] The structure of the molecular mixture can be unstable against phase separation into single-molecular domains. This instability is controlled by the strength of the cohesive interactions associated with $E_{pp}^{(1)}$ and $E_{pp}^{(2)}$ relative to the adhesive interactions associated with $E_{mp}^{(1)}$ and $E_{mp}^{(2)}$. This trade-off can be simplified by assuming that $E_{pp}^{(1)}\approx E_{pp}^{(2)}=E_{coh}$ and $E_{mp}^{(1)}\approx E_{mp}^{(2)}=E_{\mathrm{adh}}$, which reduces the number of fit parameters down to 2.

In Figs. 1 and 2, we show the predicted structures with high symmetry molecular ordering in order to compare with the illustrated experimental images. The pure PTCDA domain in Fig. 1(b) and the pure melamine domain in Fig. 1(e) are both the result of the binding rules and the high enough binding energies to ensure thermal stability of the structures.

TABLE I. (Color online) Summary of binding rules and energies in the PTCDA-melamine system. Abbreviations: mm=(melamine-melamine), pp=(PTCDA-PTCDA), and mp=(melamine-PTCDA).

Type	Bond type	Energy (eV)	Arrangement	Energy range
mm	$2\times$N-H$\cdots$O	$E_{\mathrm{mm}}=0.45$[a]		Reference value
mp$^{(1)}$	N-H$\cdots$O	$E_{\mathrm{mp}}=E_{adh}=0.225$	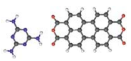	$0.2\ \mathrm{eV}<E_{adh}<0.25\ \mathrm{eV}$
mp$^{(2)}$	N-H$\cdots$O	$E_{\mathrm{mp}}=E_{adh}=0.225$	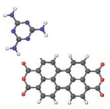	$0.2\ \mathrm{eV}<E_{adh}<0.25\ \mathrm{eV}$
pp$^{(1)}$	$2\times$C-H$\cdots$O	$E_{\mathrm{pp}}=E_{coh}=0.15$	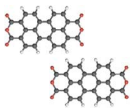	$0.1\ \mathrm{eV}<E_{coh}<0.3\ \mathrm{eV}$
pp$^{(2)}$	$2\times$C-H$\cdots$O	$E_{\mathrm{pp}}=E_{coh}=0.15$	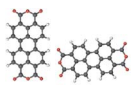	$0.1\ \mathrm{eV}<E_{coh}<0.3\ \mathrm{eV}$

[a]Reference 29.

The stability of the PTCDA-melamine structure requires a certain range of adhesive interaction energies for given values of the cohesive interaction energies, as illustrated in Fig. 3.

In Figs. 3(a)–3(f), we show how the structure undergoes a change, caused by varying the PTCDA-melamine interaction strengths $E_{mp}^{(1)}=E_{mp}^{(2)}=E_{\mathrm{ad}}$. We observe that values of $E_{\mathrm{ad}}=0.175$ eV and $E_{coh}=E_{pp}^{(1)}=E_{pp}^{(2)}=0.15$ eV lead to the phase separation due to the weak PTCDA-melamine interactions, whereas $E_{\mathrm{ad}}=0.2$ eV creates structures with long range ordering and a sporadic but reproducible occurrence of double melamine row defects. Figure 4 highlights that these double-row defects in the PTCDA-melamine domains are observed in STM [Figs. 2(a) and 4(a)] and are also predicted by our simulation [Fig. 4(c)]. It can be seen from Fig. 4(b) that both experiment [Fig. 4(a)] and simulation [Fig. 4(c)] topologically correspond. Reproducing the double-row defect in our simulations allows the range for the effective energy parameters to be narrowed, as given in Table I.

The interaction energy values we found allow all three experimentally observed structures shown in Figs. 1 and 2 to be simultaneously simulated, as illustrated in Figs. 1(b), 1(e), and 2(c). The obtained energies E_{ad} and E_{coh} comprise the contributions from both the hydrogen bonds and van der Waals interactions. The latter energies are usually in the range of 0.04–0.1 eV,[18] which is around the lower limit of the variation range identified for the parameters E_{ad} and E_{coh}. Hence, the major contribution to the obtained values of E_{ad} and E_{coh} can be associated with the hydrogen bond energies.

By combining STM images of molecular ordering in a PTCDA-melamine system with on-lattice Monte Carlo simulations of the structural stability, we have determined the molecular binding energies. We have decomposed the molecular interactions into adhesive and cohesive parts, which reduces the number of free parameters and hence the uncertainty in the energy values. The results provide information that can be used as a starting point for more detailed studies of molecular bonding using more sophisticated calculation techniques. This procedure of extracting the molecular binding rules and estimating binding energies is applicable to a wide range of multicomponent systems.

The authors thank the EPSRC (Grants Nos. EP/D048761/1 and GR/S15808/01) for funding and Chris Spencer (JEOL UK) for valuable technical support.

*f.n.silly@rug.nl

†victor.burlakov@materials.ox.ac.uk

[1] J. V. Barth, Annu. Rev. Phys. Chem. **58**, 375 (2007).

[2] G. P. Lopinski, D. D. M. Wayner, and R. A. Wolkow, Nature (London) **406**, 48 (2000).

[3] H. L. Zhang, W. Chen, L. Chen, H. Huang, X. S. Wang, J. Yuhara, and A. T. S. Wee, Small **3**, 2015 (2007).

[4] F. Silly, A. Q. Shaw, K. Porfyrakis, G. A. D. Briggs, and M. R. Castell, Appl. Phys. Lett. **91**, 253109 (2007).

[5] V. Dusastre, Nature (London) **406**, 31 (2000).

[6] P. T. Tanev and T. J. Pinnavaia, Science **267**, 865 (1995).

[7] D. S. Deak, F. Silly, K. Porfyrakis, and M. R. Castell, J. Am. Chem. Soc. **128**, 13976 (2006); Nanotechnology **18**, 075301 (2007).

[8] L. Chen, W. Chen, H. Huang, H. L. Zhang, J. Yuhara, and A. T. S. Wee, Adv. Mater. (Weinheim, Ger.) **20**, 484 (2008).

[9] J. A. Theobald, N. S. Oxtoby, M. A. Phillips, N. R. Champness, and P. H. Beton, Nature (London) **424**, 1029 (2003).

[10] F. Silly, A. Q. Shaw, G. A. D. Briggs, and M. R. Castell, Appl. Phys. Lett. **92**, 023102 (2008).

[11] D. Bonifazi, A. Kiebele, M. Stöhr, F. Cheng, T. Jung, F. Diederich, and H. Spillmann, Adv. Funct. Mater. **17**, 1051 (2007).

[12] E. Winfree, F. R. Liu, L. A. Wenzler, and N. C. Seeman, Nature (London) **394**, 539 (1998).

[13] J. V. Barth, G. Costantini, and K. Kern, Nature (London) **437**, 671 (2005).

[14] R. Otero, M. Schöck, L. M. Molina, E. Lagsgaard, I. Stensgaard, B. Hammer, and F. Besenbacher, Angew. Chem., Int. Ed. **44**, 2270 (2005).

[15] F. Silly, A. Q. Shaw, M. R. Castell, and G. A. D. Briggs, Chem. Commun. (Cambridge) **2008**, 1907.

[16] K. J. Franke, G. Schulze, N. Henningsen, I. Fernández-Torrente, J. I. Pascual, S. Zarwell, K. Rück-Braun, M. Cobian, and N. Lorente, Phys. Rev. Lett. **100**, 036807 (2008).

[17] T. Yokoyama, S. Yokoyama, T. Kamikado, Y. Okuno, and S. Mashiko, Nature (London) **413**, 619 (2001).

[18] S. Grimme, J. Comput. Chem. **25**, 1463 (2004).

[19] J. S. Swabrick, B. L. Rogers, N. R. Champness, and P. H. Beton, J. Phys. Chem. B **110**, 6110 (2006).

[20] M. M. Conn and J. Rebek, Chem. Rev. (Washington, D.C.) **97**, 1647 (1997).

[21] E. A. Archer, H. Gong, and M. J. Krische, Tetrahedron **57**, 1139 (2001).

[22] L. J. Prins, D. N. Reinhoudt, and P. Timmerman, Angew. Chem., Int. Ed. **40**, 2382 (2001).

[23] R. E. A. Kelly and L. N. Kantorovich, Surf. Sci. **589**, 139 (2005).

[24] R. E. A. Kelly, Y. J. Lee, and L. N. Kantorovich, J. Phys. Chem. **109**, 11933 (2005).

[25] F. Silly, FABVIEWER, URL: http://dr-silly.atspace.com/

[26] T. Moriuchi and T. Hirao, Chem. Soc. Rev. **33**, 294 (2004).

[27] T. Schmitz-Hubsch, T. Fritz, F. Sellam, R. Staub, and K. Leo, Phys. Rev. B **55**, 7972 (1997).

[28] W. Xu, M. Dong, H. Gersen, E. Rauls, S. Vazquez-Campos, M. Crego-Calama, D. N. Reinhoudt, I. Stensgaard, E. Laegsgaard, T. R. Linderoth, and F. Besenbacher, Small **3**, 854 (2007).

[29] U. K. Weber, V. M. Burlakov, L. M. A. Perdigão, R. H. J. Fawcett, P. H. Beton, N. R. Champness, J. H. Jefferson, G. A. D. Briggs, and D. G. Pettifor, Phys. Rev. Lett. **100**, 156101 (2008).

[30] S. K. M. Henze, O. Bauer, T.-L. Lee, M. Sokolovski, and F. S. Tautz, Surf. Sci. **601**, 1566 (2007).